Electrical Power and Energy Systems 121 (2020) 106075

Contents lists available at ScienceDirect

Electrical Power and Energy Systems

journal homepage: www.elsevier.com/locate/ijepes

Impact of wind capacity share, allocation of inertia and grid configuration on transient RoCoF: The case of the Croatian power system

Josip Đaković*, Matej Krpan, Perica Ilak, Tomislav Baškarad, Igor Kuzle

Department of Energy and Power Systems, University of Zagreb Faculty of Electrical Engineering and Computing, Zagreb, Croatia

ARTICLE INFO

Keywords:
Centers of Inertia
Low-inertia power system
RoCoF
Transient stability
Grid configuration
Wind integration
Power electronics penetration

ABSTRACT

Increased wind energy penetration influences the power system dynamic response to transient disturbances. Replacement of conventional production units with converter-connected wind turbines reduces natural power system inertia contained in rotational masses of synchronously connected turbine-generator units, therefore creating low-inertia power systems. Such a transition has an adverse effect on system resilience to disturbances and on the capability to maintain stable operation. This research examines the impact of high regional wind power production on system transient stability in the case of island operation of the Croatian power system. The system is divided into four geographical areas modeled as four centers of inertia with aggregated parameters. The study investigated initial transient RoCoF values in different areas for current and future wind capacity share scenarios, loading data, and primary frequency regulation settings. The modeling and scenario analysis have been performed on a detailed phasor power system model in the MATLAB/Simulink environment.

1. Introduction

Modern power systems are experiencing a transformation from conventional to renewable energy sourced generation which changes the overall system transient dynamics. Conventional power plants contribute to the power system stability with a large amount of kinetic energy synchronously connected to the grid [1]. Renewable energy sources (RES) such as wind and solar power plants mainly interface with the power system through frequency converters. However, these converters are often controlled in a manner that decouples generating plants from system frequency disturbances, resulting in reduced power system inertia. i.e., the ability of a system to oppose frequency deviations [2]. In the power systems with a low share of RES, wind plants produce variable power output according to available wind conditions. If their total share is small, such stochastic power sources have not been considered important in maintaining power system stability [3].

Nowadays, due to environmental and economic issues, converter-connected renewable sources rapidly displace conventional (synchronous) generators, reaching significant production shares, which open many concerns regarding power system operation and stability. Synchronous generators have an instantaneous natural response on frequency deviations, due to high kinetic energy stored in rotating masses, while modern converter-based wind turbine generators (WTG) cannot provide the same response due to converter limitations [4]. Hence, wind power involvement in frequency response is undoubtedly a necessary measure to preserve reliability in modern power systems [5]. As converter-connected power sources do not provide inherent frequency (inertial) response to active power disturbances, an advanced wind turbine control will be necessary to emulate frequency response [6].

In literature, the concept of emulated wind turbine frequency response is referred to as the Synthetic (Virtual) Inertia, or Virtual Synchronous Generator concept [7]. The research in the field of low-inertia system transient dynamic and advanced wind power plant (WPP) control methods for participating in frequency response is ongoing. As the WPP frequency response is still rarely required by transmission system operators [8], limited sets of operating experience data is available. Thus, research in the field is based on computer models with case-dependent accuracy and standardized test systems.

In this paper, the transient dynamic response of the low-inertia

Abbreviations: CoI, Centers of Inertia; DFIG, Doubly-Fed Induction Generator; EM, Electromagnetic; FFR, Fast frequency response; GE, General Electric; HPP, Hydropower plants; OS, Osijek; PF, Power factor; PP, Power plants; PMSG, Permanent Magnet Synchronous Generator; RES, Renewable energy sources; RI, Rijeka; RoCoF, Rate of Change of Frequency; RKE, Rotational kinetic energy; ST, Split; TPP, Thermal power plants; WF, Wind farm; WT(G), Wind turbine (generator); ZG, Zagreb

* Corresponding author.
E-mail addresses: josip.djakovic@fer.hr (J. Đaković), matej.krpan@fer.hr (M. Krpan), perica.ilak@fer.hr (P. Ilak), tomislav.baskarad@fer.hr (T. Baškarad), igor.kuzle@fer.hr (I. Kuzle).

https://doi.org/10.1016/j.ijepes.2020.106075
Received 26 May 2019; Received in revised form 13 March 2020; Accepted 3 April 2020

multi-machine power system with different shares of wind production capacity has been analyzed. Therefore, the focus is on quantifying the impact of concentrated wind power production in specific areas, the electrical distance among centers of inertia (CoI) and the effectiveness of two different grid topologies on initial after-transient RoCoF. The Croatian power system in island operation is used as a test example of a low-inertia high-wind penetrating system with concentrated wind production in the coastal region. Hence, this paper aims to provide insights into the current and future capabilities of the Croatian power system to maintain transient stability in island operation.

2. Paper contribution

Previous research mostly used simplified multi-area power systems dynamic models, that have not been calibrated on actual power system values. Therefore, this paper contributes to the previous research with the quantification of concentrated wind power generation impact on transient initial RoCoF with considered centers of inertia (CoI) concept in the case of the Croatian power system. The impact of two grid topologies (radial and loop), the electrical distance among CoI, realistic current and possible future operating scenarios of the Croatian power system have been considered in calculating initial transient RoCoF at four centers of inertia and its dependence on disturbance location.

In the following paragraph, a literature review of some recent papers dealing with relevant issues is presented.

2.1. Literature review

In [9], an extensive review of the frequency response services procurement from wind turbines in the case of the United States is addressed, namely technical, regulatory and economic concerns for high wind penetration levels. Also, paper reviews recent frequency response standards and requirements for wind generation in the United States. On the other side, a review of a turbine manufacturer's technology upgrades options for preservation of power system stability is also provided. A more recent review on the same issue is available in [10] covering a comprehensive overview in this field. Additionally, future research technical challenges and general recommendations are provided.

Recently there has been many virtual inertia schemes for employing kinetic energy stored in rotational masses of variable speed wind turbines (VSWT), mostly based on doubly-fed induction generator (DFIG) in frequency support participation, using various techniques such as particle swarm optimization [11], dynamic equation-based scheme and fuzzy logic-based schemes [12], variable droop gain schemes [13] and conventional de-loading levels calculations [14], coordinated control strategies between wind, various RES and energy storage (ES) systems [15,16].

In [12] comprehensive comparative analysis of virtual inertia control schemes based on dynamic equation-based scheme and the adaptive fuzzy-based scheme is tested on the PMSG and DFIG wind systems using Matlab/Simulink platform. An over-frequency mitigation issue by the usage of DFIG wind systems in low-inertia systems is addressed in [13]. The paper uses the novel variable gain control strategy to provide frequency response services and to minimize the impact on wind power dispatch. The scheme is tested, and the results indicate that it can harness more wind energy than the conventional constant droop gain schemes. An interesting approach using the particle swarm optimization algorithm is given in [11] which employs fast control response of the VSWT to inject additional power for short duration after the disturbance. Paper validates the algorithm by simulation results which show that approach limits the frequency fall while reducing post disturbances.

The procurement of inertial and primary frequency regulation capability from VSWT is analysed in [14] where a novel integrated frequency governor is proposed to provide a temporary inertial response and continued primary frequency regulation (PFR). Paper validates simulation results on an experimental platform consisting of two synchronous generators and one DFIG-based wind turbine. Results showed that the DFIG wind turbine can provide the temporary virtual inertial response and primary frequency regulation to improve the dynamic frequency stability in low-inertia systems. A similar analysis has been done in [17] where the DFIG frequency response was validated on a simple test system with one type of synchronous generators. In [18] a simplified model of DFIG with fast frequency response and primary frequency response capabilities was used for assessing the impact on power system dynamics. The wind turbine frequency support effectiveness was demonstrated on simple, linearized models in [19,20]. In [21] the WT control strategy to mitigate the impacts of reduced system inertia was investigated on the large power system considering electrical distances. The share of wind power production was assumed to be less than 1% of total production which is not relevant for wind generation and low-inertia analyses considering expected future RES penetrations of 20% and higher.

In [22], some insights of WindINERTIA® WT control function are presented, but without detailed model description. Island operation of the simple power system, consisting of diesel generator and effectiveness of DFIG WT frequency response control is presented in [23]. The impact of grid topology and synchronous inertia on multi-area power system stability has been investigated in [24,25], but each area was represented by a simple single-machine equivalent. The impact of different DFIG parameters on the frequency response of a simple two-machine system has been analyzed in [26,27,28].

In [29] a frequency response of a low-inertia power system was assessed in the case of Hawaiian and South Australia power systems. However, used model configuration and results are not clear and seem to be oversimplified for such analysis.

Requirements for synthetic and synchronous inertia amount to maintain selected RoCoF criteria are presented in [30]. Still, modeling of the considered power system is not presented in details and spatial distribution of inertia is not considered.

In [31] the operational experience of the first fast response service is reported for mitigating the frequency and angle stability in the Icelandic power system which is exposed to large frequency deviations due to its low inertia and large loads.

In this paper, we have attempted to construct a model that as accurately as possible simulates current state and possible future changes of the Croatian power system and investigates transient stability capabilities in terms of initial RoCoF.

This paper is organized into four sections. In Section 2 the research methodology with a representative model of the Croatian power system is presented. Section 3 presents and describes analyzed scenarios and discuses obtained results. The conclusion is given in Section 4.

3. Methodology

3.1. Croatian power system

The Croatian power system is a part of ENTSO-E CE interconnection and by size is one of the smallest systems in Europe. Together with Slovenia and Bosnia and Herzegovina, it constitutes the control block SLO-HR-BIH within ENTSO-E association [8]. Currently, the total approved production capacity of Croatian power plants is 5177 MW, of which 2115 MW in 26 hydropower plants (HPP), 2367 MW in 7 thermal power plants (TPP), including half of the capacity of co-owned NPP Krško, 576 MW in 19 wind power plants (WPP) and the rest of capacity consists photovoltaics (~50 MW) and ~50 MW distributed generation (DG) [32]. General geographical locations of power plants (HPPs, TPPs, and WPPs) is shown in Fig. 1. The Croatian power system is divided into four transmission areas: Split (ST), Rijeka (RI), Zagreb (ZG), and Osijek (OS). All WPPs are scattered in near-the-coast regions (RI and ST area), while conventional plants are positioned all over the country; HPPs are

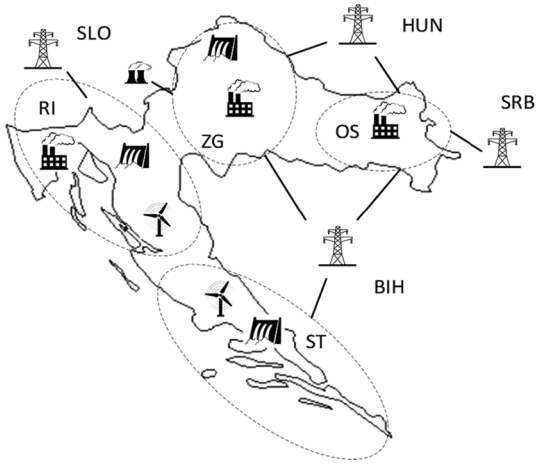

Fig. 1. Geographical position of different types of power plants in Croatia [33]

in ST, RI, and ZG areas, while TPPs are in RI, ZG and OS areas. The lowest concentra-tion of production units is in the eastern OS area, where only thermal and small DG units are positioned.

In recent years, a lot of new wind power turbines were installed, raising many questions regarding system stability and operation, due to the rapid displacement of conventional power plants from production plans. Hence, the situations where wind power plants cover more than 20% of the domestic load can be observed. Therefore, the example of a Croatian power system can be used to study the impact of high wind power production on the frequency dynamics of a power system with reduced inertia.

3.2. Model

For this research, a three-phase phasor model of the Croatian electric power system in island operation was developed in the MATLAB/Simulink environment (Fig. 2). The main idea for model developments was to present all power plants of the same type in the area as one production unit with aggregated parameters. The model incorporates the concept of Centers of Inertia (CoI) which assumes that all available system inertia in a region is concentrated in one grid node. The CoI concept was first introduced in [34] where the contribution of DFIG in short-term frequency control was investigated.

Power plants of the same type in a region are presented as one production unit connected to the belonging CoI bus directly or over a short line (Fig. 2). CoI-s are connected via three-phase π-section line blocks to include spatial distance among the areas in two different manners (Fig. 2): (a) radial configuration; (b) loop configuration. Radial

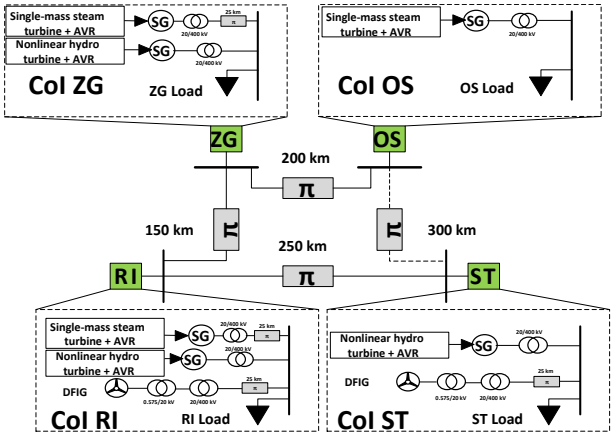

Fig. 2. The four-area concept of the Croatian power system.

Table 1
Line parameters.

Parameter	Positive sequence	Zero sequence
Resistances (Ohms/km)	0.0114	0.2894
Inductances (H/km)	0.00086	0.0034
Capacitances (F/km)	1.342e-8	8.588e-9

configuration simulates complete separation from neighboring power systems, while loop configuration assumes a fictional connection between ST and OS across the BIH. Used transmission line parameters are shown in Table 1, while line lengths are marked in Fig. 2. Additionally, each region has own consumption block, modeled as a switchable three-phase RLC load. The voltage level of the transmission grid is selected to be 400 kV.

3.3. Conventional power plants

Hydropower plants (3 units) and thermal power plants (3 units) are modeled as three-phase synchronous machines with IEEE Type 1 excitation system, driven by hydro or thermal turbine model with a speed governor. Thermal power plants are modeled with a single mass shaft model. All synchronous generators are connected to the CoI bus through their own 20/400 kV step-up transformer (Fig. 2). Each component is a part of the SimPowerSystem library in Matlab/Simulink software. For simplicity, default electrical parameters of synchronous machines have been used, except for power capacities, inertia constants, and speed governor settings, which are parameterized according to actual plants' operational data and available TSO data [35].

Parameters of conventional production units, used in this study, are shown in Table 2. Production capacities are varied according to tables Tables 3–6 in the Scenario Analysis section. Area-based inertia constants H of different types of power plants were calculated as the ratio of a weighted sum of individual generator inertia constants and the maximum capacity of generating units of the same type currently available in individual areas as follows [33,36]:

$$H_{area} = \frac{\sum_{i=1}^{n} S_i H_i}{\sum_{i=1}^{n} S_i} \quad (1)$$

where S_i is the capacity of i-th considered plant (MVA), H_i is inertia constant of i-th plant and n is the total number of plants in the area. The numerator of Eq. (1) presents total rotational kinetic energy (RKE) of synchronously connected power plants in the area. Additionally, system-based inertia constant for each group of generators is calculated with the base capacity of 1000 MVA (Table 2) to gain insight into available inertia in each area. Also, system-based inertia constant is used as a weighting factor in calculating frequency and RoCoF (see Eqs. (3) and (4)). Regulator droop R was selected according to actual primary regulation settings and controller characteristics reported by TSO. In this paper, TPPs have not been used for frequency regulation, i.e. they have constant active power reference. Speed governors of HPPs (PID regulators) were parametrized to imitate the actual gate opening speed of Croatian plants which participate in primary regulation.

Table 2
Parameters of conventional production units [33]

Area	ST		RI		ZG	OS
	HPP	*TPP*	*HPP*	*TPP*	*HPP*	*TPP*
H (s) (area based)	3.59	4.16	2.88	4.21	1.68	4.93
H (s) (system based)	4.96	2.52	1.36	5.16	0.44	0.48
Droop R (%)	4	–	4	–	4	–
Max gate opening speed (p.u./s)	0.1	–	0.036	–	0.1	–
Active power reference (p.u.)	0.65	0.85	0.8	0.85	0.75	0.85

Table 3
Base case.

Total capacity (MVA)	ST	RI	ZG	OS	Σ (%)
TPP	–	500	650	100	**1250 (36.44)**
HPP	750	600	250	–	**1600 (46.65)**
WPP	540	40	–	–	**570 (16.91)**
Load	800-j90	750-j90	950-j90	350-j5	**2850-j275**

Table 4
Wind25 case.

Total capacity (MVA)	ST	RI	ZG	OS	Σ (%)
TPP	–	120	600	100	**820 (24.40)**
HPP	750	700	250	–	**1700 (50.60)**
WPP	540	300	–	–	**840 (25.00)**
Load	800-j90	750-j90	950-j90	350-j5	**2850-j275**

Table 5
Wind30 case.

Total capacity (MVA)	ST	RI	ZG	OS	Σ (%)
TPP	–	–	400	100	**500 (15.38)**
HPP	750	750	250	–	**1750 (53.85)**
WPP	550	450	–	–	**1000 (30.77)**
Load	800-j90	750-j90	950-j90	350-j5	**2850-j275**

Table 6
Wind40 case.

Total capacity (MVA)	ST	RI	ZG	OS	Σ (%)
TPP	–	–	100	50	**150 (4.69)**
HPP	850	670	250	–	**1700 (55.31)**
WPP	550	730	–	–	**1280 (40.00)**
Load	800-j90	750-j90	950-j90	350-j5	**2850-j275**

3.4. Wind farms

Wind farms located in ST and RI areas are modeled as one equivalent scaled Simulink phasor model component of a Doubly-Fed Induction Generator (DFIG) driven by a 1.5 MW wind turbine [37], connected to the belonging CoI bus through the 0.575/20 kV and 20/400 kV step-up transformers (Fig. 2).

Almost all Croatian wind farms are comprised of variable speed Type 3 (DFIG) and Type 4 (Full-converter). According to [6,38], Type 3 and Type 4 wind turbines do not provide any (or provide negligibly) inherent inertial response without special controls. This justifies using only DFIG based turbine models to simplify analysis and decrease calculation time. Nominal wind turbine mechanical power (MW), generator rated electrical power (MVA) and nominal converter DC bus capacitance (mF) of a wind turbine model component have been scaled with the factor k [37], denoting the number of turbines in each area:

$$k = \frac{Total\ \ WPP\ \ capacity\ \ in\ \ area\ \ (MVA)}{1.5\ \ MW/0.95\ \ PF} \tag{2}$$

where denominator means rated generator power (MVA) at 0.95 power factor. The average WTG power in the Croatian power system is 2.5 MW, but it does not affect results as the total capacity of wind turbines is only important for system stability assessments. Total WPP capacities simulated in this study are listed in tables Tables 3–6. Wind speed was set to the rated 12 m/s to drive WT on nominal parameters.

4. Scenario analysis

The scenarios are chosen to map possible changes in production capacities shares in the Croatian power system. The main intention was to simulate grid response on the wind power capacity integration and reduction of conventional power plants production capacity, mainly TPP. Four different wind capacity scenarios have been successfully simulated on both radial and loop grid configuration. The total load in simulations, which represent a high load scenario for the Croatian power system, was the same in each considered scenario.

The base scenario simulates current conditions in the Croatian grid with ~17% wind power capacity (Table 3). Then, wind capacity was increased to ~25%, reducing the on-line TPP capacity which are most likely to phase out in the nearby future (Table 4). On-line HPP capacity is assumed to increase in some areas, as Base case does not consider all available plants to be on-line. The next two scenarios, Wind30 (Table 5), and Wind40 (Table 6) are formulated with a similar pattern as the second scenario, increasing the total wind capacity by 5% in each scenario. A further increase in wind capacity has not been considered in this paper since it would mean decommissioning HPPs which is not realistic for our case.

Area-based inertia constants of synchronous power plants were kept the same in all scenarios for simplicity (Table 2). HPPs were modeled with an active power reference signal in the range 0.65–0.8 p.u. of nominal capacity, while thermal power plants were modeled with 0.85 p.u. (Table 2). Due to its slow active power change speed, TPPs speed regulators were overridden in all scenario, thus only HPPs participated in frequency regulation after disturbance. Operation of WPPs was simulated at rated capacity with 0.95 PF before the disturbance. To induce a large system disturbance, 250 MW load (~10% of total load) is switched-on alternately at different CoI buses in the simulations.

5. Results

The overall simulation lasted for 100 sec, while load disturbance occurs in 50th sec. After the transient, the system is taken over by primary frequency regulation which started to stabilize the frequency. The main transient stability parameter considered in this paper is the initial rate of change of frequency (RoCoF) as it only depends on the physical inertia of the system. Maximum initial RoCoF values of filtered signal (measured within 5 ms after the disturbance) are reported in 'heatmap' tables (Fig. 3) for both radial and loop grid configuration. The impact of additional power line in loop configuration on RoCoF values is marked with red and green color, where green fields mark reduction of (absolute) RoCoF, and red fields mark increase when compared to radial configuration. Due to numerical calculation instabilities (RoCoF signal noises) and variable simulation time-steps for different cases, reported results may deviate from the actual values due to a statistical error in signal processing. Time-domain plots of unfiltered RoCoF values in ST and RI areas are shown in Figs. 4 and 5.

RoCoF values were calculated as derivations of local frequencies at each CoI as follows [34]:

$$f_{CoI} = \frac{H_{HPP}f_{HPP} + H_{TPP}f_{TPP}}{H_{HPP} + H_{TPP}} \tag{3}$$

$$RoCoF_{CoI} = \frac{df_{CoI}}{dt} \tag{4}$$

where H_{HPP} and H_{TPP} present system-based inertia constants of HPPs and TPPs (Table 2); f_{HPP} and f_{TPP} presents calculated rotor frequencies of aggregated HPP and TPP models and f_{CoI} present average weighted frequency of synchronous machines [38].

As the ST area has only HPP with synchronous inertia, the ST frequency was calculated as the rotor frequency of the aggregated HPP model. Similarly, OS area frequency is the rotor frequency of TPP located in that area. The time-domain plot of system frequency in the Base case measured in ST and OS CoI, for disturbance in different CoIs, is shown in Fig. 6.

Adding a new line caused an increase of voltage levels in the system

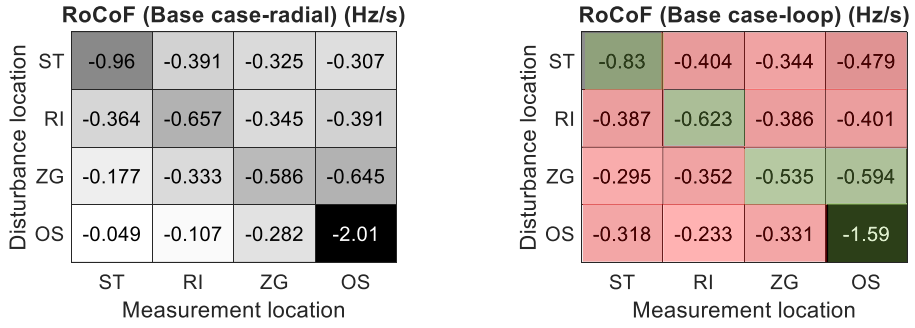

Avg (RoCoF) = -0.495 Hz/s
Std (RoCoF) = 0.463

Avg (RoCoF) = -0.506 Hz/s
Std (RoCoF) = 0.325

a) Base case - radial and loop configuration

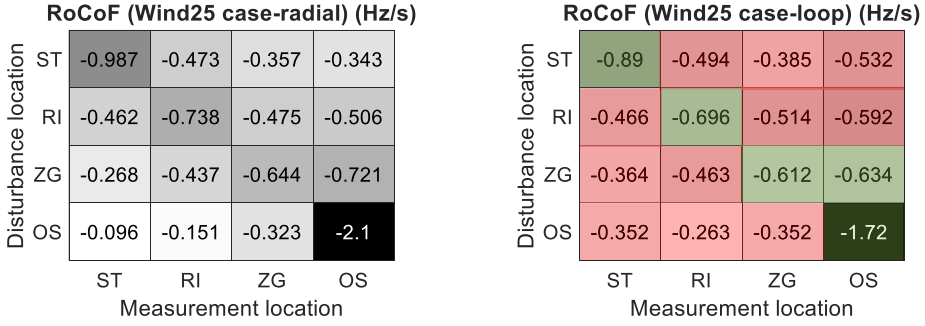

Avg (RoCoF) = -0.567 Hz/s
Std (RoCoF) = 0.467

Avg (RoCoF) = -0.583Hz/s
Std (RoCoF) = 0.341

b) Wind25 case - radial and loop configuration

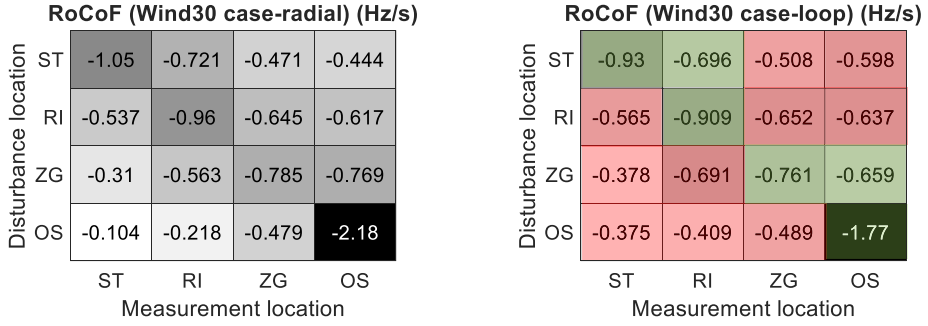

Avg (RoCoF) = -0.676 Hz/s
Std (RoCoF) = 0.471

Avg (RoCoF) = -0.689 Hz/s
Std (RoCoF) = 0.332

c) Wind30 case - radial and loop configuration

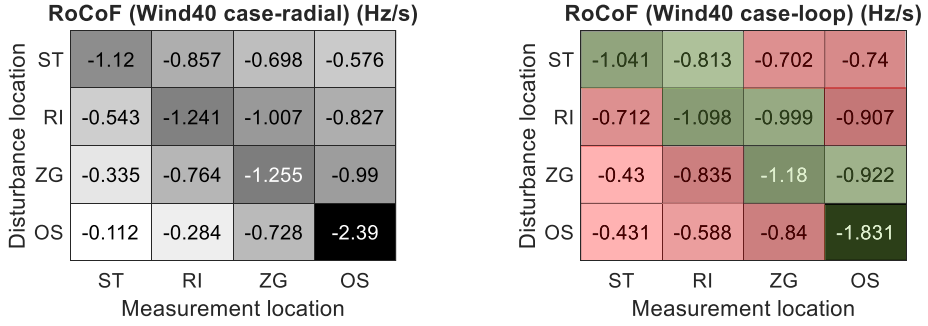

Avg (RoCoF) = -0.857 Hz/s
Std (RoCoF) = 0.526

Avg (RoCoF) = -0.879 Hz/s
Std (RoCoF) = 0.333

d) Wind40 case - radial and loop configuration

Fig. 3. Initial RoCoF values in CoIs: (a) Base case; (b) Wind25 case; (c) Wind35 case; (d) Wind40 case.

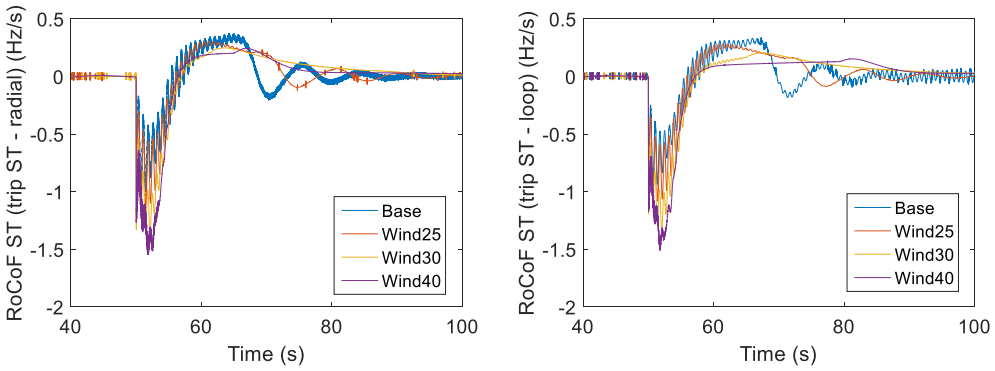

Fig. 4. RoCoF in ST for different scenarios (disturbance in ST) (raw data): (a) radial; (b) loop.

for ~0.3% and an increase of overall active load for ~0.7%, as the load is modeled as constant impedance, with square dependence of applied voltage. Furthermore, higher initial voltage levels in loop configuration induced ~3% higher disturbance (disturbance load is pure active power constant impedance load) than in radial configuration.

6. Discussion

In Fig. 3 the initial RoCoF in each of CoI is shown for different disturbance locations and for two different grid configurations, i.e. the radial case and the loop case (mashed). The wind capacity share is varied from base level of ~17% to 25%, 30%, and 40%, also changing the capacities of HPP and TPP, to examine effects of wind penetration on the initial RoCoF.

1. Generally, the rule is that no matter where the fault location is and where the measured RoCoF is the initial RoCoF deteriorates as wind penetration levels increase (Fig. 3). Also, initial RoCoF directly depends on the amount of inertia in CoI, i.e. CoI like OS which has the lowest production capacity and the lowest inertia in all cases, has the highest RoCoF values when the disturbance is in that CoI.
2. The first thing to notice in Fig. 3 is that the average RoCoF in the meshed grid increases. The reason for this is that adding a new power line between OS and ST CoIs increased active power disturbance (3% higher disturbance) due to increased system voltages (which is the consequence of higher reactive power production of this low-loaded line) and constant impedance of disturbance load. This is noticeable for all cases of wind penetration.
3. The second thing to notice in Fig. 3 is that the standard deviation of RoCoF decreases in the meshed grid. The reason for this is that meshing the grid causes the initial RoCoF in all CoIs to converge toward the average system RoCoF, dependent on fault location, as can be observed for all wind penetration cases and fault locations. This means the peak values of RoCoF in low inertia CoIs are decreased (flattened) by adding a new power line.
4. Another observation in Fig. 3 is that adding a new power line would mostly improve the initial RoCoF in CoI where disturbance occurs (green diagonal). The reason for this is the before-mentioned convergence of RoCoF in all CoIs to the average value, and since the location of fault has the highest initial RoCoF then the average improvement is higher.
5. Off-diagonal values of RoCoF in the looped grid increased (marked with red color in Fig. 3) because of the before-mentioned phenomena of convergence towards the average level of RoCoF. This happened because of better electrical interconnection of CoIs which enabled higher inertial support to other locations at its own expense. Exception from this is the RoCoF in OS CoI when the disturbance is in ZG CoI (Base case and Wind25 case). In that case, RoCoF in OS is higher or similar to one in ZG (value higher than system average), due to its low inertia and electrical proximity to ZG CoI. As the grid meshing flattens RoCoF towards average, loop configuration decreases OS RoCoF for the disturbance in ZG in all cases. Decreasing off-diagonal RoCoF in loop configuration in Wind30 and Wind40 case in RI and ZG CoI can be explained by the same facts.

In Fig. 6, the time-domain plot of system frequency measured in ST and OS CoIs is shown for different fault locations and for the Base case scenario. A similar pattern occurs in all wind penetration scenarios.

1. It can be observed that meshing the grid aims to converge the family of frequencies into a single curve. The reason for this is increased admittance of the grid and lower line congestions.
2. Furthermore, average nadir is increased in meshed configuration due to before mentioned 3% increased active power disturbance.
3. On the other hand, the standard deviation of the nadir is lower in the meshed grid (convergence of frequency functions).
4. The addition of a new line cannot improve average system frequency nadir as can be seen in Fig. 6. The reason for this is that

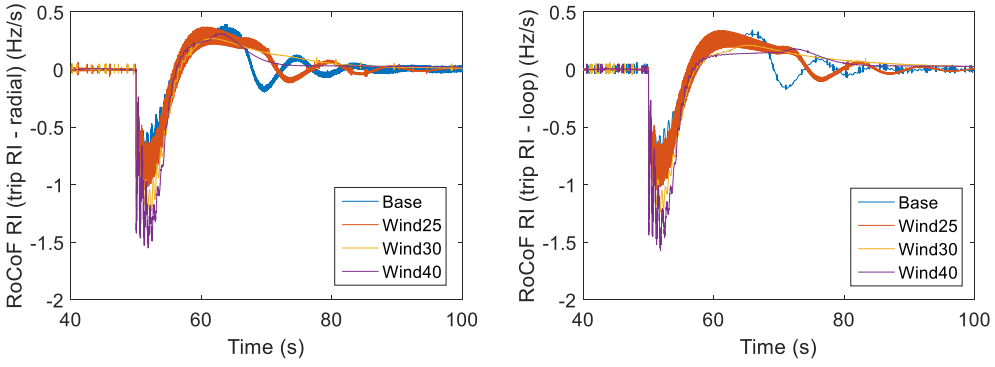

Fig. 5. RoCoF in RI for different scenarios (disturbance in RI) (raw data): (a) radial; (b) loop.

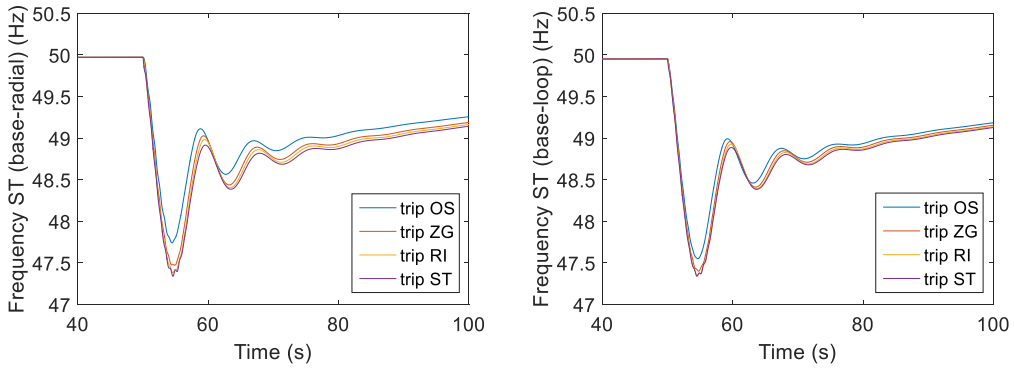

a) Frequency at ST - radial and loop configuration

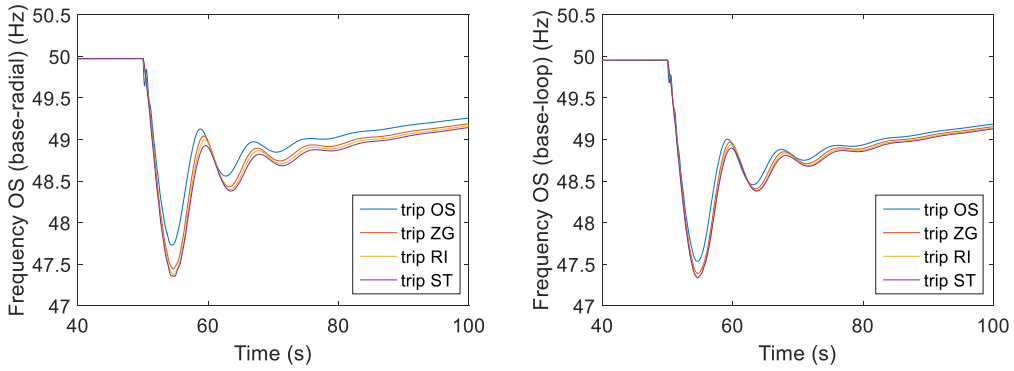

b) Frequency at OS - radial and loop configuration

Avg Base case (Nadir-radial) = 47.631 Hz
Std (Nadir) = 0.172

Avg Base case (Nadir-loop) = 47.549 Hz
Std (Nadir) = 0.097

Fig. 6. System frequency for disturbances in different CoIs: (a) frequency at ST; (b) frequency at OS.

meshing the grid does not add any new sources of inertia, but only increases the connection between existing sources. In order to improve nadir, new inertial capacity should be introduced, the speed of primary regulation response should be increased and spinning reserve capacity and allocation should be optimized.

5. Interesting observation; when disturbance happens in CoI with lowest system-based inertia constant (OS CoI) which also has the highest electrical distance to the neighboring CoIs, maximum system frequency deviation tends to be the lowest (blue curve in Fig. 6). This is less pronounced in meshed grid configuration than in radial. The actual explanation for that phenomenon is a combination of multiple factors: electrical distance, total capacity share (inertia), spinning reserve allocation, primary regulation settings, etc., which is out of the scope of this paper, focusing primarily on initial RoCoF values.

7. Conclusions

In this paper, the impact of different wind penetration levels, electrical distance and grid configuration on initial RoCoF values in the four-area (four CoI) power system, based on the Croatian power system, are examined.

It can generally be concluded that adding a new line in a power system aims to equalize initial RoCoF in all CoIs, i.e. shift towards the average value occurring after the disturbance in a specific location. A significant benefit from that fact can have low-inertia power system areas, whose stability will highly depend on interconnection with the rest of the system. However, additional grid meshing cannot decrease the average initial RoCoF, as it only depends on available on-line inertia in the system.

Regarding system frequency nadir, it can be observed that in meshed (loop) grid configuration, deviation between family of system frequency curves for different disturbance locations is smaller, meaning that the disturbance location has less impact on the frequency trajectory after the disturbance. Furthermore, meshing the grid could not improve the average frequency nadir for a specific disturbance. Also, disturbances electrically distanced from high inertia CoIs have a smaller effect on system frequency degradation. However, when a grid is more meshed, that is less noticeable.

In this paper, system protection measures (like under-frequency load shedding-UFLS or RoCoF relays) have not been considered, thus showed frequency curves are unrealistic for actual power systems, as the frequency nadir would be restricted to much higher values. However, insight in initial RoCoF values shows the amount of system stability reduction, important for system protection planning, as the wind power penetrates is the system, phasing out conventional plants.

CRediT authorship contribution statement

Josip Đaković: Conceptualization, Methodology, Investigation, Writing - original draft, Writing - review & editing. **Matej Krpan:** Conceptualization, Methodology, Writing - review & editing. **Perica Ilak:** Conceptualization, Methodology, Writing - original draft, Writing - review & editing, Supervision. **Tomislav Baškarad:** Writing - review & editing. **Igor Kuzle:** Conceptualization, Methodology, Writing - review & editing, Supervision.

Declaration of Competing Interest

The authors declare that they have no known competing financial

interests or personal relationships that could have appeared to influence the work reported in this paper.

Acknowledgment

This work has been supported in part by the Croatian Science Foundation under the project WINDLIPS – WIND energy integration in Low Inertia Power System (Grant No. HRZZ-PAR-02-2017-03) and in the part by Horizon 2020 project CROSSBOW–CROSS Border management of variable renewable energies and storage units enabling a transnational Wholesale market (Grant No. 773430). This document has been produced with the financial assistance of the European Union. The contents of this document are the sole responsibility of authors and can under no circumstances be regarded as reflecting the position of the European Union.

References

[1] Nesje B. The need for Inertia in the Nordic Power System. Norwegian University of Science and Technology; 2015.
[2] ENTSO-E AISBL. Future system inertia. Brussels, 2015.
[3] Miller NW, Clark K. Advanced Controls Enable Wind Plants to Provide Ancillary Services. In: IEEE PES General Meeting, Providence, RI, USA, July 2010.
[4] Miller NW, Clark K, Shao M. Frequency responsive wind plant controls: Impacts on grid performance. In: IEEE Power and Energy Society General Meeting, Detroit, MI, USA, July 2011.
[5] Brisebois J, Aubut N. Wind Farm Inertia Emulation to Fulfill Hydro-Québec's Specific Need. In: IEEE Power and Energy Society General Meeting, Detroit, MI, USA, 2011.
[6] National Renewable Energy Laboratory; University of Colorado; Electric Power Research Institute. Active Power Controls from Wind Power: Bridging the Gaps. NREL, January 2014.
[7] Rezkalla M, Pertl M, Marinelli M. Electric Power System Inertia: Requirements, Challenges and Solutions. Electr Eng 2018;100(4):2677–93.
[8] Windlips project. Power regulation and grid inertia report. 2019. [Online]. Available: http://windlips.com/wp-content/uploads/2019/02/Power-regulation-and-grid-inertia-report.pdf. [Accessed 2019].
[9] Singarao YV, Rao SV. Frequency responsive services by wind generation resources in United States. Renew Sustain Energy Rev March 2016;55:1097–108.
[10] Attya A, Dominguez-Garcia JL, Anaya-Laraa O. A review on frequency support provision by wind power plants: Current and future challenges. Renew Sustain Energy Rev 2017;81:2071–87.
[11] Hafiz F, Abdennou A. Optimal use of kinetic energy for the inertial support from variable speed wind turbines. Renew Energy 2015;80:629–43.
[12] Pradhan C, Bhende CN, Samanta AK. Adaptive virtual inertia-based frequency regulation in wind power systems. Renew Energy 2018;115:558–74.
[13] Li Y, Xu Z, Zhang J, Wong KP. Variable gain control scheme of DFIG-based wind farm for over-frequency support. Renew Energy 2018;120:379–91.
[14] Fu Y, Zhang X, Hei Y, Wang H. Active participation of variable speed wind turbine in inertial and primary frequency regulations. Electr Power Syst Res June 2017;147:174–84.
[15] Li Y, He L, Liu F, Tan Y, Cao Y, Luo L, Shahidehpou M. A dynamic coordinated control strategy of WTG-ES combined system for short-term frequency support. Renew Energy 2018;119:1–11.
[16] Mishra S, Sharma R, Sharma D. Coordinated active power control of Wind, Solar and Diesel Generator in a Microgrid. In: 9th IFAC Symposium on Control of Power and Energy Systems CPES 2015, New Delhi, 2015.
[17] Bhatt P, Long C, Jianzhong Wu BM. Dynamic Participation of DFIG for Frequency Regulation in Electrical Power Systems. Energy Procedia 2017;142:2183–8.
[18] Ochoa D, Martinez S. Fast-Frequency Response Provided by DFIG-Wind Turbines and its Impact on the Grid. IEEE Trans Power Syst 2017;32(5):4002–11.
[19] Krpan M, Kuzle I. Inertial and primary frequency response model of variable-speed wind turbines. J Eng 2017;13:844–8.
[20] Krpan M, Kuzle I. Linearized model of variable speed wind turbines for studying power system frequency changes. In: IEEE EUROCON 2017, Ohrid, 2017.
[21] Gautam D, Goel L, Ayyanar R, Vittal V, Harbour T. Control strategy to mitigate the impact of reduced inertia due to doubly fed induction generators on large power systems. IEEE Trans Power Syst 2011;26(1):214–24.
[22] Singhvi V, Pourbeik P, Bhatt N, Brooks D, Zhang Y, Gevorgian V, et al. Impact of wind active power control strategies on frequency response of an interconnection. In: IEEE Power & Energy Society General Meeting, Vancouver, BC, Canada, July 2013.
[23] Kayikci M, Milanovic JV. Dynamic Contribution of DFIG-Based Wind Plants to System Frequency Disturbances. IEEE Trans Power Syst 2009;24(2):859–67.
[24] Ulbig A, Borsche TS, Andersson G. Analyzing Rotational Inertia, Grid Topology and their Role for Power System Stability. IFAC-PapersOnLine 2015;48:541–7.
[25] Ulbig A, Borsche TS, Andersson G. Impact of low rotational inertia on power system stability and operation. IFAC Proceedings Volumes (IFAC-PapersOnline) 2014;47:7290–7.
[26] Krpan M, Kuzle I, Liu Y. Analysing Frequency Support from DFIG-based Wind Turbines-Impact of Parameters and Initial Conditions. In: 1th Mediterranean Conference on Power Generation, Transmission, Distribution and Energy Conversion, Cavtat, 2018.
[27] Krpan M, Kuzle I. Dynamic characteristics of virtual inertial response provision by DFIG-based wind turbines. Electric Power Syst Res 2020;178(106005).
[28] Krpan M, Kuzle I. Introducing low-order system frequency response modelling of a future power system with high penetration of wind power plants with frequency support capabilities. IET Renew Power Generation 2018;12(13):1453–61.
[29] Stenclik D, Richwine M, Miller N, Hong L. The Role of Fast Frequency Response in Low Inertia Power Systems. In: CIGRE 2018, Paris.
[30] O'Connell B, Cunniffe N, Eager M, Cashman D, O'Sullivan J. Assessment of Technologies to Limit the Rate of Change of Grid Frequency on an Island System. In: CIGRE 2018, Paris.
[31] Wilson D, Heimisson B, Gudmansson IBR, Armannsson O, Halldorsson K, Linnet E, et al. Icelandic Operational Experience of Synchrophasor-based Fast Frequency Response and Islanding Defence. In: CIGRE 2018, Paris.
[32] HOPS, Desetogodišnji plan razvoja prijenosne mreže 2018.-2027., s detaljnom razradom za početno trogodišnje i jednogodišnje razdoblje, 2017.
[33] Đaković J, Ilak P, Baškarad T, Krpan M, Kuzle I. Effectiveness of Wind Turbine Fast Frequency Response Control on Electrically Distanced Active Power Disturbance Mitigation. In: Mediterranean Conference on Power Generation, Transmission, Distribution and Energy Conversion (MEDPOWER), Dubrovnik, 2018.
[34] Akbari M, Madani SM. A new method for contribution of DFIG-based wind farms in power system frequency regulation. In: North American Power Symposium, Arlington, TX, USA, 2010.
[35] Kuzle I. Identification of Dynamic Parameters Relevant for Frequency Changes in Medium Developed Electric Power System. University of Zagreb; 2002. Ph.D. thesis.
[36] Sibeko B, Coller JV, Hurford G. A Dynamic Multi-Variate Approach to the Management of Power System Inertia. In: CIGRE 2018, Paris.
[37] MathWorks Documentation. Wind Farm Using Doubly-Fed Induction Generators. [Online]. Available: https://www.mathworks.com/help/physmod/sps/powersys/ug/wind-farm-using-doubly-fed-induction-generators.html. [Accessed 2019].
[38] Tielens P, Henneaux P, Cole S. Penetration of renewables and reduction of synchronous inertia in the European power system – Analysis and solutions. ASSET project, 2018.